

Complexes of Co(II), Ni(II) and Cu(II) with 2-((2-methoxybenzylidene)amino) acetohydrazide hydrate: preparation, characterization and antimicrobial activities

Fathi Mohammed Al.-azab¹, Yasmin Mos'ad Saeed Jamil*¹, Amani Ahmed Mahdi Al-Gaadbi¹, Ahmed N. Al-hakimi^{2,3}, Ibrahim A. Alhagri^{2,3}, Entesar A. H. Alhuraishi¹, S. El-Sayed Saeed²

¹Chemistry Department, Faculty of Science, Sana'a University, Sana'a, Yemen

²Department of Chemistry, College of Science, Qassim University, Qassim, Buraidah, 51452, Saudi Arabia

³Department of Chemistry, Faculty of Science, Ibb University, Ibb, Yemen

*Corresponding author: y.jamil@su.edu.ye, yasminjml@yahoo.com

Abstract

In this study, one new Schiff base hydrazide derived from 2-Methoxy benzaldehyde, glycine and hydrazine hydrate as a ligand and its transition metal complexes were synthesized. The structures of these compounds were characterized by using elemental analysis, magnetic susceptibility measurements, conductivity, molar ratio, electronic, infrared, and NMR spectra, X-ray diffraction, and antioxidant analysis. The ligand was found to be a bidentate ligand involving the imino nitrogen and the nitrogen of amine in all complexes, in addition to the oxygen of the carbonyl group in Ni^{II} complex. The metal to ligand ratios were found to be 1:1 for all of the prepared complexes. The Co(II) and Ni(II) complexes have been found in a square planar geometry, while the complex of Cu(II) has octahedral geometry. Complexes of Co(II) and Ni(II) have electrolytic nature but the complex of Cu(II) was not. The ligand and its complexes were screened for their antifungal and antibacterial activity. The results indicated that these compounds exhibited good antifungal and antibacterial activities.

Keywords: Schiff bases, hydrazides, XRD, aldehydes, antioxidant, antimicrobial

1. Introduction

1.1 Schiff Bases

A German Chemist Hugo Schiff 1864 papered Schiff base and therefore referred to his name. The majority of the Schiff bases are represented by the general formula $R_1R_2C=NR_3$, or $R_1CH=NR_2$, in which carbon is attached to a hydrogen atom instead of an alkyl or aryl group[1]. Schiff bases are derived from the condensation reaction of aromatic/aliphatic aldehydes and amines and form stable complexes with different transition metal ions that are still relevant to be of great interest in inorganic chemistry,[2] There is a continuing interest in metal complexes of Schiff bases because of the presence of both hard nitrogen or oxygen donor atoms in the backbones of these ligands. They readily coordinate with a wide range of transition metal ions yielding stable metal complexes, some of which have been shown to exhibit interesting physical and chemical properties and potentially useful biological activities[3].

1.2 Hydrazides

Groups of organic derivatives of hydrazine containing the functional active group - $C(=O)NHNH_2$ are name hydrazides and were produced as far back as 1895 by Kurzius,[4] Hydrazides behave similarly to hydrazines, because an alkyl or an acyl radical bound to the NH end of $NH-NH_2$ does not influence significantly the reactivity of the NH_2 group.[5] Hydrazides have been investigated due to their antitumour, antibacterial, antifungal, and biocidal activity. Hydrazides have been used widely as antituberculous compounds because of their ability to form metal chelates [6] hydrazides have been used widely in medicine, catalysis, and analytical chemistry. However, the use of hydrazide metal complexes to inhibit corrosion is scarce and so there is a need for a broad spectrum of hydrazide complexes to be synthesized and employed in the control of corrosion [7].

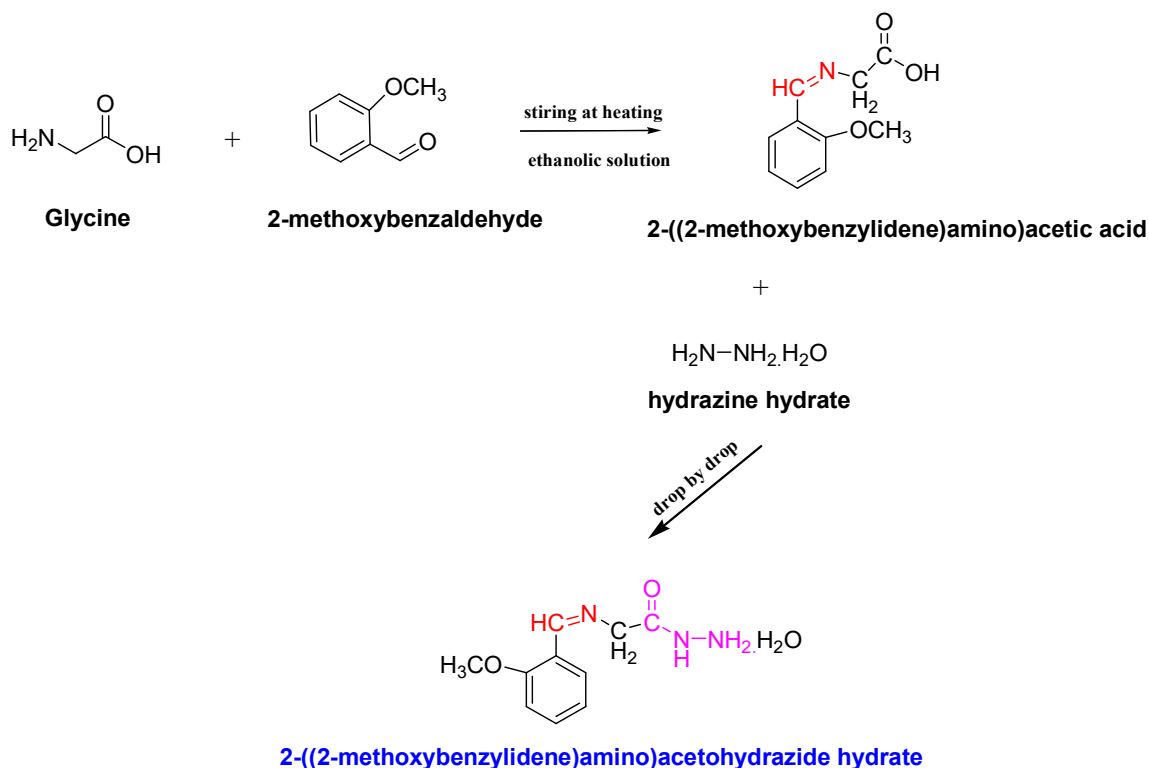
In recent years, many biologically important hydrazide derivatives with several functional groups have been synthesized from many different carbonyl compounds. They were found to possess anticancer [8-11], anti-inflammatory [12], anticonvulsant [13], antiviral [14], and antiprotozoal [15] activities. Among the biological properties of this class of compounds, antimicrobial activity is the most frequently encountered one in scientific literature. Additionally, widely used chemotherapeutic agents such as nitrofurazone [16], furazolidone [17,18], and nitrofurantoin [19,20] are known to contain specific hydrazide–hydrazone moiety or hydrazide-hydrazone moiety. Encouraged by the facts mentioned above, this study is an attempt to prepare a schif base-hydrazide, which can be considered a potential antimicrobial agent.

2.1 Methods

All chemicals used were commercially available from BDH-UK. The melting points were determined in glass capillary tubes at degrees celsius. Molar conductance in DMSO (10^{-3} M solution at 25 °C) and molar ratio were measured on Jenway conductivity meter model 4510-UK, the ligand and its complexes were characterized by comparison of spectroscopic data, IR spectra of the ligand and metal complexes were measured by using (FT/IR – 140, Jasco, Japan) using dry KBr as the standard reference, ^1H and ^{13}C NMR spectra were recorded in a Varian FT – 300 MHz spectrometer(USA) in d_6 - DMSO solvent using TMS as internal standard, UV-Visible spectra and antioxidant activity measurements (by Ferric-bipyridine method) using (specord 200, Analytik Jena, Germany) using DMSO as the reference for UV-Visible spectra and methanol as a solvent for antioxidant activity measurements. The magnetic susceptibilities of the complexes were measured at room temperature using Gouy's method by a magnetic susceptibility balance from Johnson Metthey and Sherwood model. Carbon, hydrogen and nitrogen (CHN) were estimated by Vario ELFab. The X-ray powder diffraction patterns of the ligand and the solid complexes were obtained using XD-2(Shimadzu ED-720, Japan), X-ray powder diffractometer at a voltage of 35 KV and current of 20 mA using CuK radiation generator in the range $5^\circ < 2\theta < 70^\circ$ with a 1° min^{-1} scanning rate and a wavelength of 0.154056 nm. Microbiological analysis was carried out using the filter paper disc method [6].

2.2 Synthesis of 2-((2-methoxybenzylidene)amino)acetohydrazide hydrate = (Ligand)

The solid ligand was prepared in 1:1:1 molar ratio by adding dropwise an ethanolic solution of glycine (0.01mol) to an ethanolic solution of the aldehyde 0.01mol with stirring. The mixture was refluxed for 3 hours with constant stirring and heating[21] until a light brown solution of the Schiff base is formed. Then added hydrazine hydrate drop by drop to the hot solution of the Schiff base with constant stirring until a light brown precipitate is formed. The resulting precipitate was filtered off and washed with ethanol till the solution become clear then left to dry.



2. 3 Synthesis of the solid transition metal complexes

The solid complexes were prepared by adding dropwise a methanolic solution of the hydrated metal chlorides (0.008mol) to a methanolic solution of the ligand (Schiff base hydrazide 0.008 mol) with stirring. The mixture of each was refluxed for 4 to 6 hours with constant stirring until colored precipitates are formed. All the materials solutions were in 1:1 molar ratios. The resulting precipitates were filtered off and washed with methanol even becoming a clear solution, then left them to dry.

3. Results and Discussion

The solubility of colored solids compounds is recorded in (Table 1). The molar conductance values of Co^{II} and Ni^{II} complexes were 142 and 176 $\text{mho cm}^2\text{mol}^{-1}$, respectively, indicating their electrolytic nature. Cu^{II} complex was 9.01 indicating its non-electrolyte [22]. Values are recorded in (Table 2).

Table 1: Some physical properties of the ligand and its complexes

Comp. Proposed formula	Color	M.p /°C	Yield %	Solubility											
				H ₂ O	EtOH	MeOH	Hex	CC ₄	CHCl ₃	Acet .	Benz.	D.E.	DMF	DMSO	
L (C ₁₀ H ₁₅ N ₃ O ₃)	Apple green	173	88.41	Ins	p.s	S	S	S	S	S	S	S	Ins	S	S
[Co (L)(H ₂ O) ₂]Cl ₂ [Co(C ₁₀ H ₁₇ N ₃ O ₄)]Cl ₂	dirty brown	250	71.55	S	S	S	Ins	Ins	Ins	Ins	Ins	p.s	Ins	p.s	S
[Ni (L) H ₂ O]Cl ₂ [Ni(C ₁₀ H ₁₅ N ₃ O ₃)]Cl ₂	Olive green	285	54.69	S	S	S	Ins	Ins	Ins	Ins	Ins	Ins	Ins	p.s	S
[Cu (L)(H ₂ O) ₂]Cl ₂ [Cu(C ₁₀ H ₁₇ N ₃ O ₄)]Cl ₂	Light brown	201	72.31	Ins	Ins	p.s	p.s	S	S	S	S	S	Ins	S	S

Table 2: Molecular weight, elemental analysis , and molar conductance of the ligand and its complexes

Complex proposed formula	Molecular weight		Elemental analysis										Am- cm ² mol ⁻¹ Ω ⁻¹	
			%C		%H		%N		%M		%Cl			
			Calc.	found	Calc.	found	Calc.	found	Calc.	found	Calc.	found		Calc.
L	225.24	225.27	53.32	53.31	6.71	6.72	18.66	18.65	-	-	-	-	-	-
[Co (L)(H ₂ O) ₂]Cl ₂	373.10	373.18	32.19	32.19	4.59	4.62	11.26	11.26	15.80	15.79	19.01	19.04	142	
[Ni (L) H ₂ O]Cl ₂	354.84	354.90	33.85	33.85	4.26	4.29	11.84	11.84	16.54	16.55	19.98	19.98	176	
[Cu (L)(H ₂ O) ₂]Cl ₂	377.71	377.76	31.80	31.79	4.54	4.57	11.13	11.12	16.82	16.81	18.77	18.79	9.01	

3.1 Molar ratio by conductivity measurements

The molar ratio between the free ligand and the divalent metals, Co^{II}, Ni^{II} and Cu^{II}, by the conductivity measurements were used as shown in (Figure 1) and as the following points:

1. Concerning the Co^{II} and Ni^{II} complexes, they gave high conductivity values, which indicates that these complexes have ionic properties, and this was proven using silver nitrate, Through the resulting values, it was found that the ratio between chloride and metals is 2:1[22]
2. As for the molar conductivity values of the Co^{II} and Ni^{II} complexes, indicated that the molar ratio between the ligand and these metals is 1:1, by confirming the conductivity reading at this molar ratio [23].
- 3- The conductivity value of the Cu^{II} complex was low, which indicates that this complex does not have an ionic nature, the conductivity values of the different molar concentrations of this complex were fixed at a certain value, which indicates that the ratio between the ligand and copper is 1:1 [24].

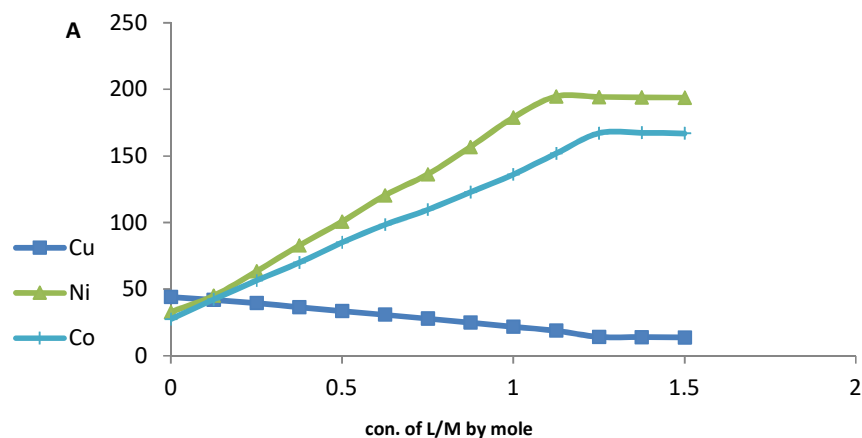


Figure 1 : Curve of mole ratio for the ligand and metals

3.2 IR Spectra of the ligand and its complexes

The IR spectra of the complexes were compared with this of the free ligand (Table 3 and Figure 2)in order to determine the coordination sites that may be involved in chelating. In complexes of Co^{II} and Cu^{II} , the ligand acts as bidentate through C=N and NH_2 , resulting in a decrease of the C=N stretching frequency[25] and NH_2 stretching frequency[26]. While the ligand acts as a tridentate molecule, through C=N, C=O, and NH_2 groups with Ni^{II} ,The presence of a broad band at $3422\text{-}3448\text{ cm}^{-1}$ is ascribed to the stretching vibration of OH[27][25]. The new stretching vibration observed in the lower frequencies which was noticed at about $(580\text{-}584)\text{ cm}^{-1}$ and $(419\text{-}424)\text{ cm}^{-1}$ attributed to M-N and M-O bands, respectively [27]. Another band observed at 402 cm^{-1} in the Cu^{II} complex is attributed to M-Cl[28]. Also there are bands (e.g. $\nu(\text{CH}_3)$ [27], $\nu(\text{C}=\text{O})$ [27], $\nu(\text{CH})$ [29] , $\nu(\text{C-O-C})$ [29] [30], $\nu(\text{C}=\text{C})$ [30] listed in (Table 3)

Table 3 : Significant IR spectral bands (cm^{-1}) of the ligand and its complexes

Comp.	C=N	C=O	C=C	C-N	NH	NH_2	=C-H	N-N	CH_3	CH_2	C-O-C	H_2O	M-O	M-N M-Cl
L	1663 ^w	1671 ^w	1599 ^s	1437 ^s	3002 ^m	3185 ^w	3050 ^w	1044 ^s	2965 ^m	1466 ^s	1249 ^s	3448 ^{br}	-	-
$[\text{Co}(\text{L})(\text{H}_2\text{O})_2]\text{Cl}_2$	1638 ^m	1675 ^w	1599 ^s	1437 ^s	3003 ^m	3074 ^m	3048 ^w	1044 ^s	2959 ^w	1466 ^s	1249 ^s	3422 ^{br}	424 ^w	582 ^m -
$[\text{Ni}(\text{L})(\text{H}_2\text{O})]\text{Cl}_2$	1615 ^s	1684 ^s	1599 ^s	1438 ^s	3004 ^m	3075 ^m	3045 ^w	1045 ^s	2965 ^w	1467 ^s	1249 ^s	3386 ^{br}	422 ^w	584 ^m -
$[\text{Cu}(\text{L})(\text{H}_2\text{O})_2]\text{Cl}_2$	1637 ^w	1675 ^m	1602 ^s	1438 ^m	3003 ^w	3020 ^w	3042 ^w	1048 ^m	2960 ^w	1459 ^s	1251 ^s	3448 ^{br}	4419 ^m	580 ^m 402 ^w

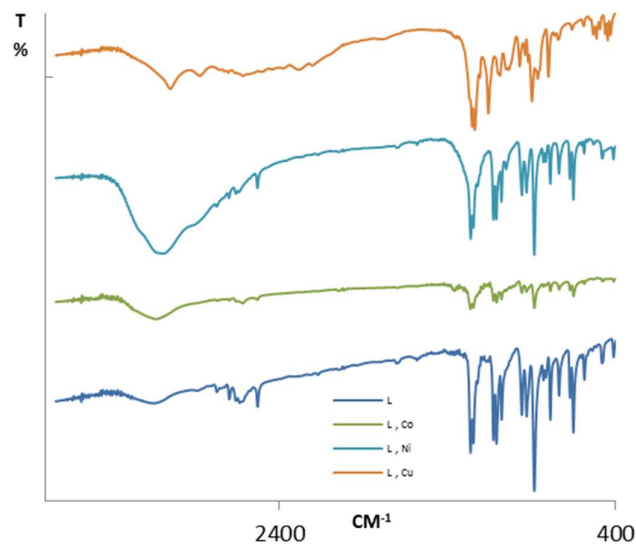


Figure 2 : IR spectra of the ligand and its complexes

3.3 NMR Spectroscopy

3.3.1 ¹H NMR

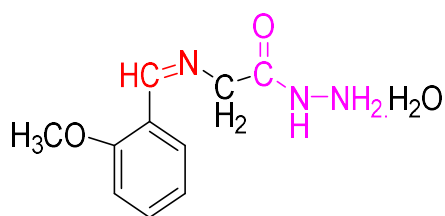
The ¹H-NMR. Spectra of free ligand (Table 4 and Figure 3) show the following signals the azomethine proton signal at 8.935 ppm[31]. The signals appear at 7.518 and 7.994 ppm due to the NH and NH₂ protons, respectively[6]. The multiplet signals in the region δ 7.015–7.150 ppm for the aromatic ring[32]. Also, the proton signal of methoxy group appeared at 3.6 ppm [33-35], while the signals at 2.5 and 3.6 ppm due to the protons of CH₂[36] and H₂O[37], respectively.

3.3.2 ¹³C NMR

The ¹³C NMR spectrum of the ligand (Table 4 and Figure 4) show signal at 156.521 ppm attributed to carbon of azomethine (-CH=N-)[37], and the signal at 158.736 ppm due to carbon of amide group[30], The multi signals in the region 111.977-132.981 ppm corresponds to the aromatic carbons of benzene ring[38][39], while the signals at 55.762 ppm and 40.026 ppm due to the carbons of methoxy and methyl groups, respectively[30].

Table 4: ¹H and ¹³C NMR positions (ppm) of the

NMR Spectroscopy of the ligand			
¹ H NMR		¹³ C NMR	
Site	Chemical Shift (ppm.)	Site	Chemical Shift (ppm.)
CH=N-	8.935	CH=N-	156.521
NH	7.518	A.R.	111.977-132.981
NH ₂	7.994	CH ₃	55.762
A.R.	7.500-7.799	C=O	158.736
CH ₂	2.5	CH ₂	40.026
CH ₃	3.878	-	-
H ₂ O	3.33	-	-



2-((2-methoxybenzylidene)amino)acetohydrazide hydrate

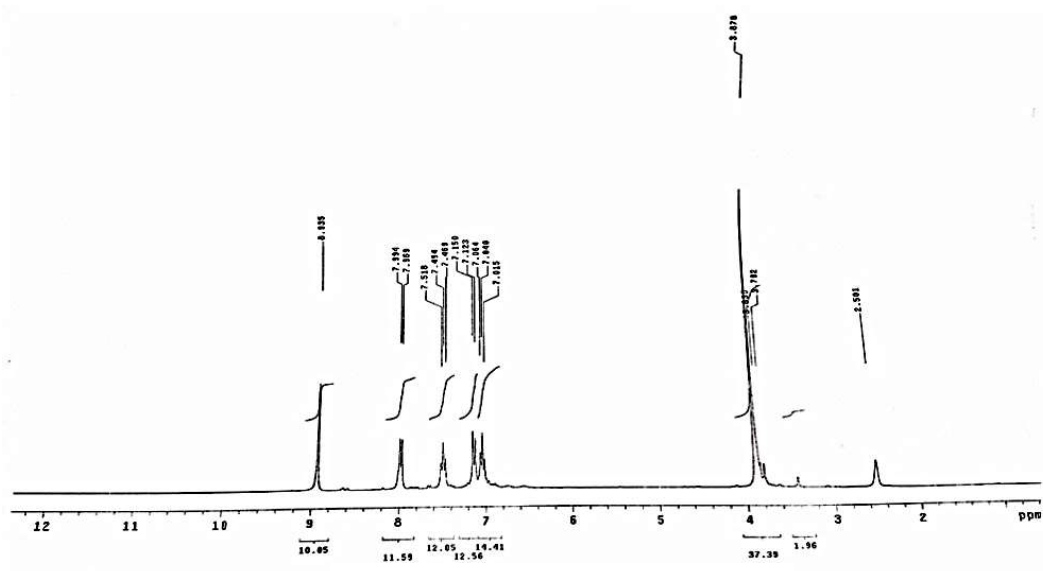


Figure 3: ¹H NMR Spectrum of the ligand

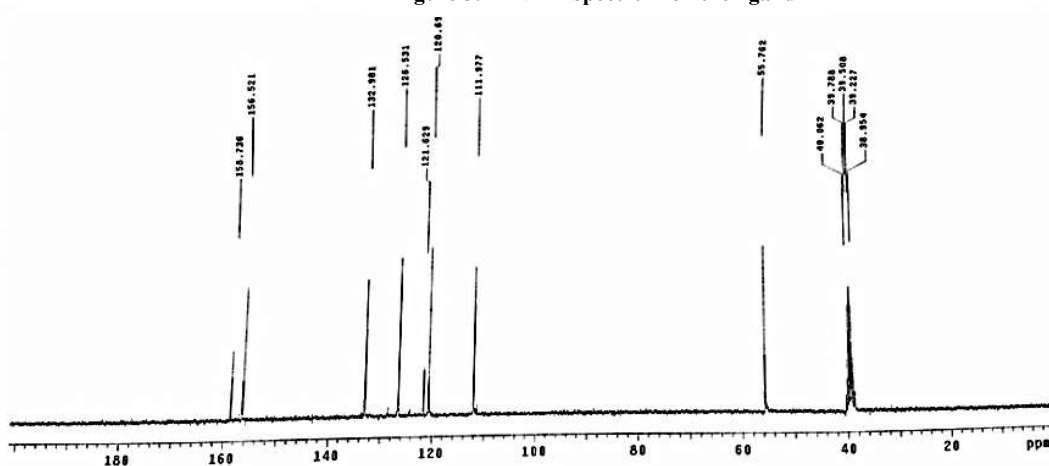


Figure 4: ¹³C NMR Spectrum of the ligand

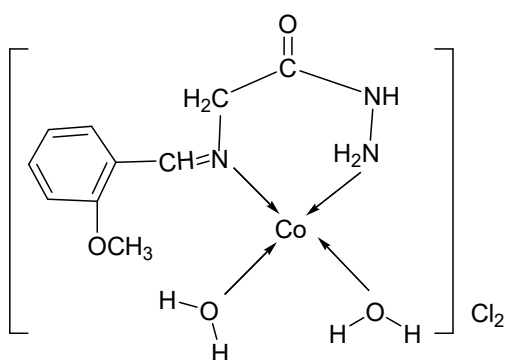
3.4 Magnetic and electronic spectrum of the ligand and its complexes

The electronic spectrum of the ligand in DMSO solution shows intense bands at 37037 cm^{-1} and 33333 cm^{-1} attributed to $\pi \rightarrow \pi^*$ and $n \rightarrow \pi^*$ transition of the benzene and non-

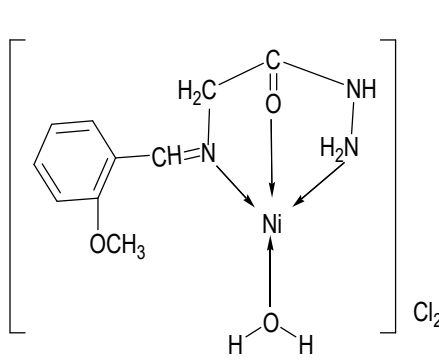
bonding electrons present on the nitrogen of the azomethine group, respectively[40]. The electronic spectrum of the Co^{II} complex has provided good evidence for the structure of this complex as shown in (Figure 5) For the following Co^{II} complex is square planar suggested. This is based on the appearance of 20408 cm^{-1} and 15873 cm^{-1} bands in the spectra recorded in DMSO solution (Table 5), Co^{II} complex has a magnetic moment of 2.6 B.M., which lies in the range reported for square planar geometry around the Co^{II} ion[41]. Moreover, the dirty brown of the complex is in good agreement with that reported for square planar Co^{II} complexes[42]. From the above discussion, one can suggest (structure 1) for Co^{II} complex. The magnetic measurement of Ni^{II} complex indicates that, the complex is diamagnetic and the electronic spectra of this complex showed two bands at 12345 cm^{-1} and 23809 cm^{-1} (Table and Figure 5), which are assigned to $^1\text{A}_{1g} \rightarrow ^1\text{A}_{2g}$ and $^1\text{A}_{1g} \rightarrow \text{B}_{1g}$ transitions, respectively (Figure 5), this supports a square planar geometry around Ni^{II} (Structure 2)[40]. The Ni^{II} complex is an olive green color which supports this structure [41]. The electronic spectra of Cu^{II} complex in DMSO solution (Figure 5) show a band at 19607 cm^{-1} this band is due to $^2\text{E}_g \rightarrow ^2\text{T}_{2g}$ transition (Table 5), on this basis a distorted octahedral geometry is suggested (Structure 3). The broadness of the observed band may be due to Jahn-Teller effect, which enhances the distortion of the octahedral geometry. The light brown color of this complex supports the proposed geometry [22]. The magnetic moment values of this complex 2.1 B.M. was found to be within the range reported for the d^9 -system containing one unpaired electron. Also an intense absorptions at the region $24691 \text{ cm}^{-1} - 23255 \text{ cm}^{-1}$ were observed in the spectra of all of the complexes were assigned to charge transfer transitions [43].

Table 5 : Magnetic moment, electronic spectral data in DMSO solution for the ligand and its Complexes

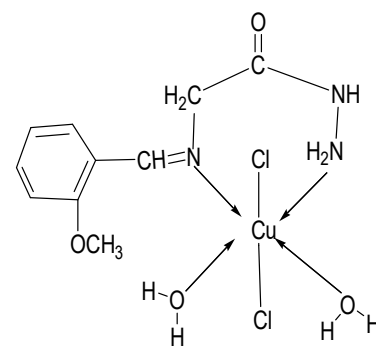
Comp.	μ_{eff} (B.M)	UV bands(cm^{-1})		Charge transfer bands (cm^{-1})	d-d transition bands (cm^{-1})	Supposed structure
		$\pi \rightarrow \pi^*$	$n \rightarrow \pi^*$			
L	-	37037	33333	-	-	-
$[\text{Co}(\text{L})2\text{H}_2\text{O}]\text{Cl}_2$	2.6	-	-	23809	20408, 15873	Square Planar
$[\text{Ni}(\text{L})\text{H}_2\text{O}]\text{Cl}_2$	dia	-	-	24691	23809, 2345	Square Planar
$[\text{Cu}(\text{L})2(\text{H}_2\text{O})\text{Cl}_2]$	2.1	-	-	23255	19607	Distorted Octahedral



Structure 1: Complex of L with Co^{II}



Structure 2: Complex of L with Ni^{II}



Structure 3: Complex of L with Cu^{II}

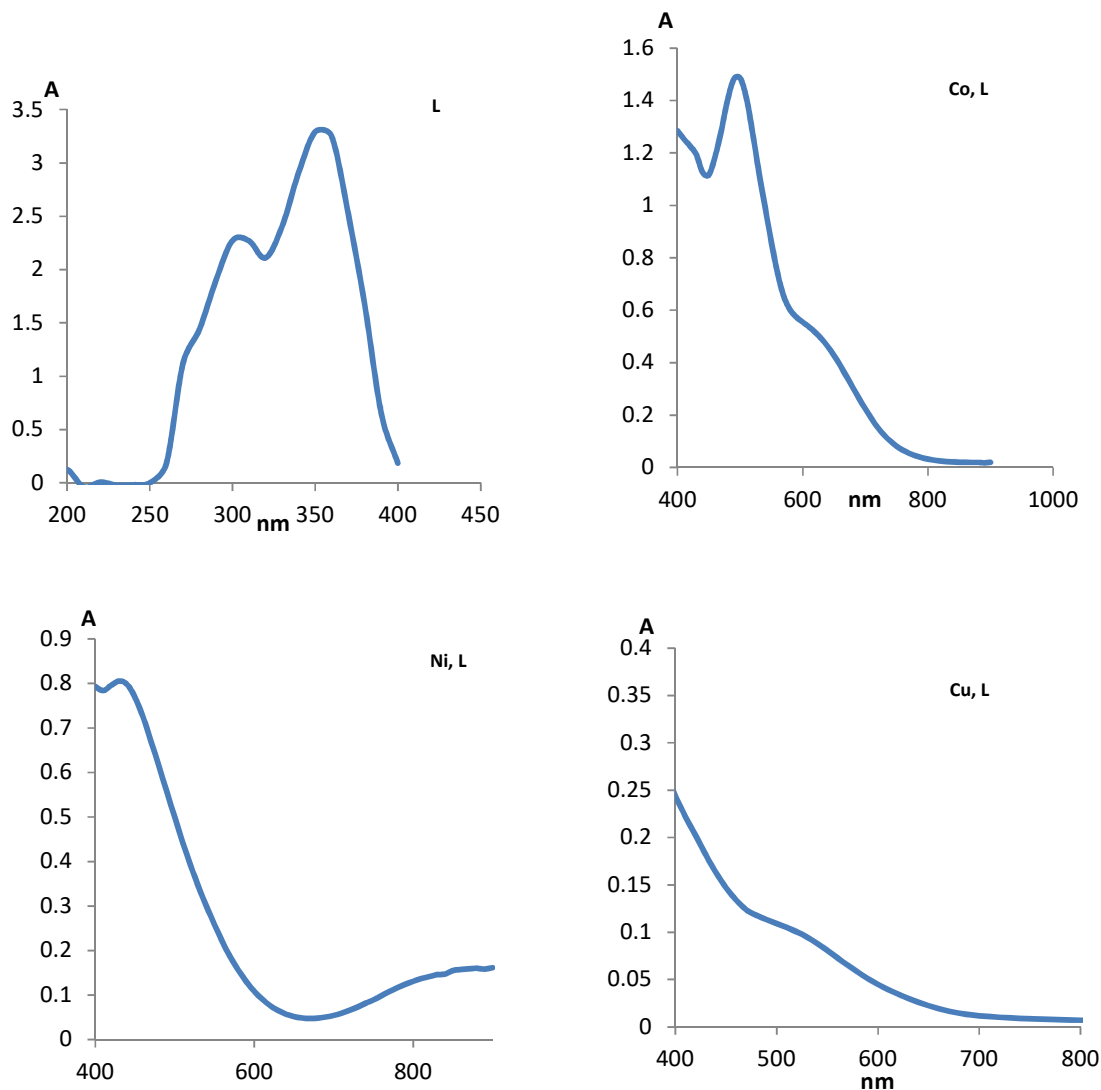


Figure 5 : UV-visible electronic spectrum of the ligand and its complexes in DMSO solution

3.5 X-ray diffraction of the ligand and its Complexes

From the X-ray analysis of the ligand and its complexes, the following factors were deduced: crystal size, crystalline strain, and crystalline ratio. The crystal size was calculated using the Scherrer equation [44-46], and the intercept of Williamson-Hall equation[47].

$$D = K\lambda / \beta \cos \theta \quad (\text{Scherrer equation})$$

$$D = K\lambda / \text{intercept} \quad (\text{Williamson-Hall equation})$$

The resulting values were in nano size (12.17 - 31.64 nm). While the strain of the ligand and Cu^{II} complex have crystalline tensile properties through the positive values that resulted, the Co^{II} and Ni^{II} complexes have a crystal compressive property and this is consistent with the resulting negative values as well as the size of the particles using William's equation [47] confirming these results as the crystal tensile values correspond to the size of the particles

larger than the size of the particles With crystal compression, and this is what was deduced from the (Figures 6 and 7) and recorded in the (Table 6).

$$\text{Strain } (\varepsilon) = \beta * \cos \theta / 4 \sin \theta$$

The percentage of crystallinity $X_c(\%)$ was calculated based on the integrated peak areas of the principal peaks[45]. The crystallinity of the complex is calculated relative to the crystallinity of the ligand as a ratio,

$$X_c(\%) = A_{\text{complex}}/A_{\text{ligand}} * 100$$

where A_{complex} and A_{ligand} are the areas under the principal peaks of the complex and the ligand sample, respectively. Where the calculations proved that the ligand has a higher crystal property than its complexes.

Table 6 : XRD spectral data of the highest value of intensity of the ligand and its complexes

Compounds	θ (Radian)	β (FWHM) (Radian)	$\beta \cos \theta$	$4 \sin \theta$	D(nm)	Mean D(nm)	W-H D(nm)	Strain (ε)*10 ⁻⁴	X%
L	0.1080	0.005864	0.005830	0.4313	24.84	22.40	25.86	9	100
	0.1909	0.006545	0.006426	0.7591	22.54				
	0.3349	0.007575	0.007154	1.3148	20.24				
	0.3897	0.007122	0.006587	1.5198	21.99				
[Co (L)2(H2O)]Cl2	0.1112	0.006877	0.006834	0.4438	21.19	31.64	20.40	-13	1.53
	0.1796	0.005009	0.004929	0.7145	29.38				
	0.3297	0.009791	0.009264	1.2950	15.63				
[Ni (L)(H2O)]Cl2	0.3787	0.002583	0.002401	1.4789	60.34	18.05	12.17	-36	9.64
	0.1124	0.010716	0.010649	0.4487	13.60				
	0.1880	0.008936	0.008779	0.7475	16.50				
[Cu (L)2(H2O) Cl2]	0.3334	0.007662	0.007240	1.3089	20.00	17.98	23.74	23	8.14
	0.3908	0.007086	0.006552	1.5236	22.10				
	0.1152	0.007819	0.007767	0.4597	18.64				
	0.1888	0.006405	0.006291	0.7509	23.02				
	0.3234	0.011170	0.01059	1.2712	13.67				
	0.3955	0.009460	0.008729	1.5410	16.59				

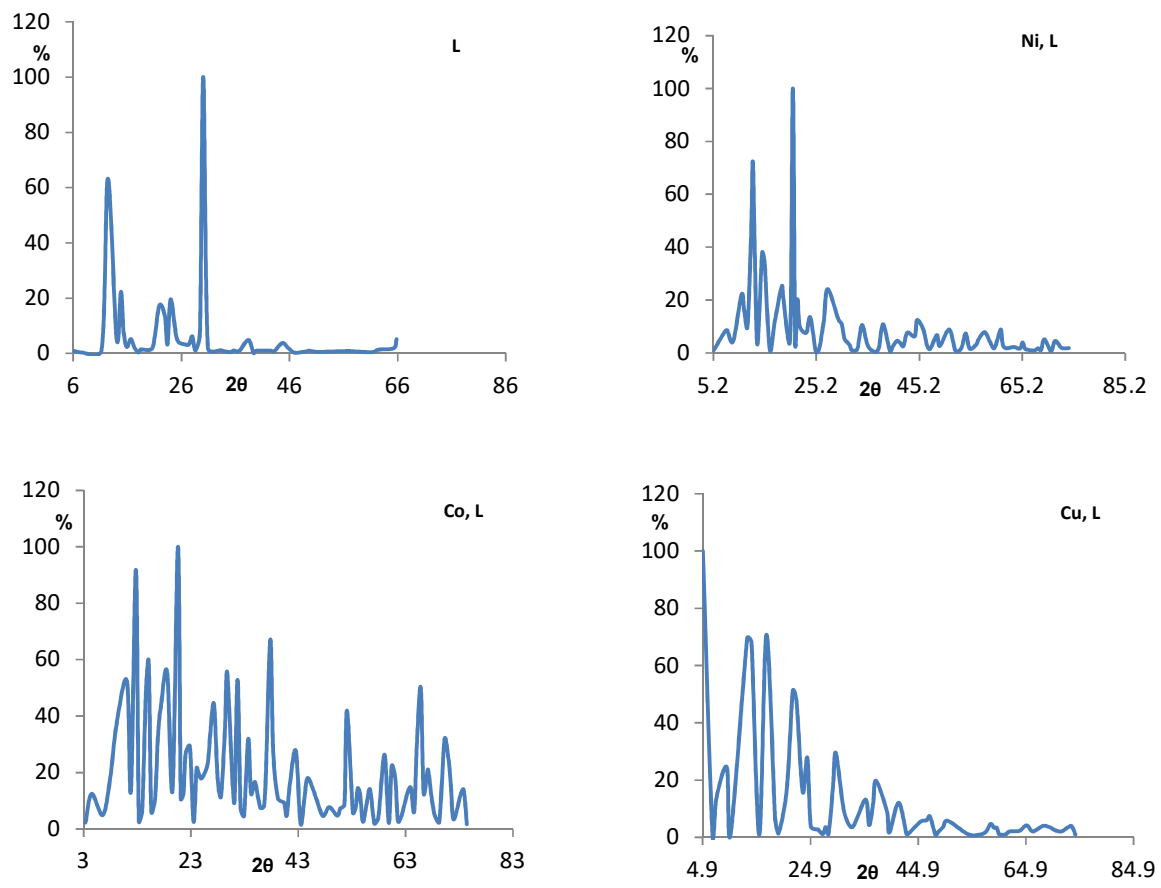


Figure 6: XRD patterns of the ligand and its complexes

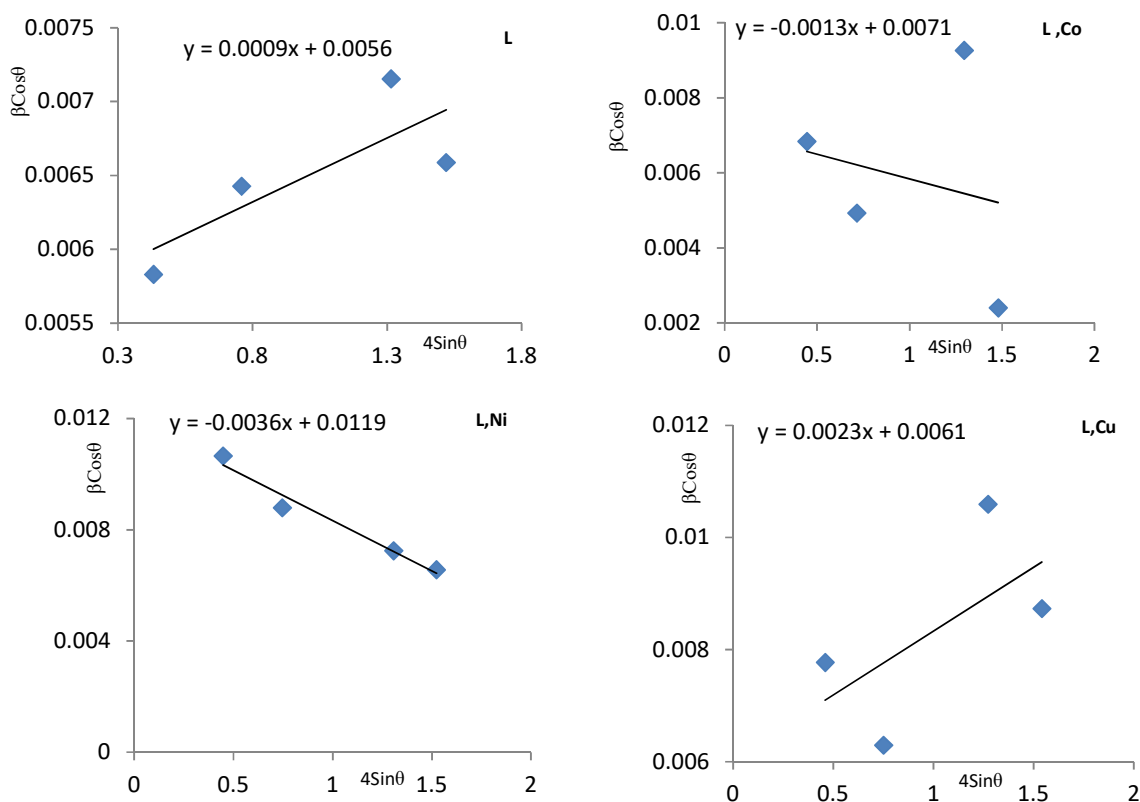


Figure 7: particle size and strain by W-H of the ligand and its complexes

3.6 Antioxidant of the ligand

Through using the FBRC method [48] compared to the antioxidant (ascorbic acid) which was used as a standard material in this analysis, the ligand was a good antioxidant which means this ligand can be used as an antioxidant, but with less effectiveness than ascorbic acid, which gave 3.3333 mg. compared with ascorbic acid which was 1mg. while the standard deviation of this ligand was $\pm 3.3 \cdot 10^{-9}$ (Table 7).

Table 7: result comparison of FBRC for determination of antioxidant

Comp.	Ascorbic acid	ligand
number of replicates	6	3
Standard deviation	$\pm 2.96222 \cdot 10^{-3}$	$\pm 3.3 \cdot 10^{-9}$
Effectiveness (mg)	1	3.3333

3.7 Antimicrobial Studies

Comparison between the biological evaluation of the ligand and its complexes with the standards Gentamicin as (an antibacterial agent) and Nystatin, Miconazole, Itraconazole, and Metronidazole as (antifungal agents) against four species of bacteria (*Staphylococcus aureus*,

Bacillus, *Escherichia coli*, *Pseudomonas aeruginosa*) and two fungal species (*Aspergillus Flavus* and *Candida albicans*) (Table 8 and illustrated in Figures 8 – 9). from these results, we can summarize that:

1. Generally, the active property of the free ligand and has complexes is enhanced.
2. The antimicrobial activity of the ligand is slightly enhanced against the *Staphylococcus aureus*, *Bacillus subtilis*, *Pseudomonas aeruginosa*, and *Candida albicans* compared to the complexes.
3. The growth of *Escherichia coli* just inhibited by complexes of Co^{II} , Ni^{II} and the ligand.
4. Inhibition zone by complex of Cu^{II} complex is less than the ligand and complexes of Co^{II} , and Ni^{II} against *Aspergillus flavus*.

Since the lipid membrane of the cell prevents the passage of non-fatty compounds, meaning it allows the passage of soluble substances since the solubility of fats is an important factor for penetrating the cell wall, the polarity of the metal ion is greatly reduced due to the overlap of the orbitals of the metal ion with the bound. It increases the delocalization of electrons on the rings and increases the fatty property in the complexes, which facilitates the penetration of the fatty membranes of microorganisms and prevents the association of the metal with enzymes. These compounds deactivate enzymes in the cell, which play an important role in the metabolism of these organisms. Meaning the denaturation of one or more cell proteins, reducing cellular processes[25][49][50].

Table 8: Effect of the ligand and its complexes on the growth of bacteria and fungi (Zone of inhibition in mm).

		Inhibition zone diameter (mm)					
		Bacteria				fungi	
		Gram positive		Gram negative		Aspergillus flavus	Candida albicans
Staphylococcus aureus	Bacillus subtilis	Pseudomonas aeruginosa	Escherichia coli				
Control DMSO		0.0	0.0	0.0	0.0	0.0	0.0
Antibacterial agent Gentamicin 120µg/ml		23	22	25	23	-	-
Standard	Nystatin 100 µg/ml	-	-	-	-	25	21
	Miconazole 50 µg/ml	-	-	-	-	8	22
	Itraconazole 30 µg/ml	-	-	-	-	18	20
	Metronidazole 5 µg/ml	-	-	-	-	10	17
L		16	13	15.3	6.5	27.5	19
[Co (L) 2H₂O]Cl₂		12	0	10	16.5	29.5	15
[Ni (L) H₂O]Cl₂		13	10.5	7	9	16.5	14
[Cu (L) 2(H₂O) Cl₂]		10	9.5	11	0	16	17

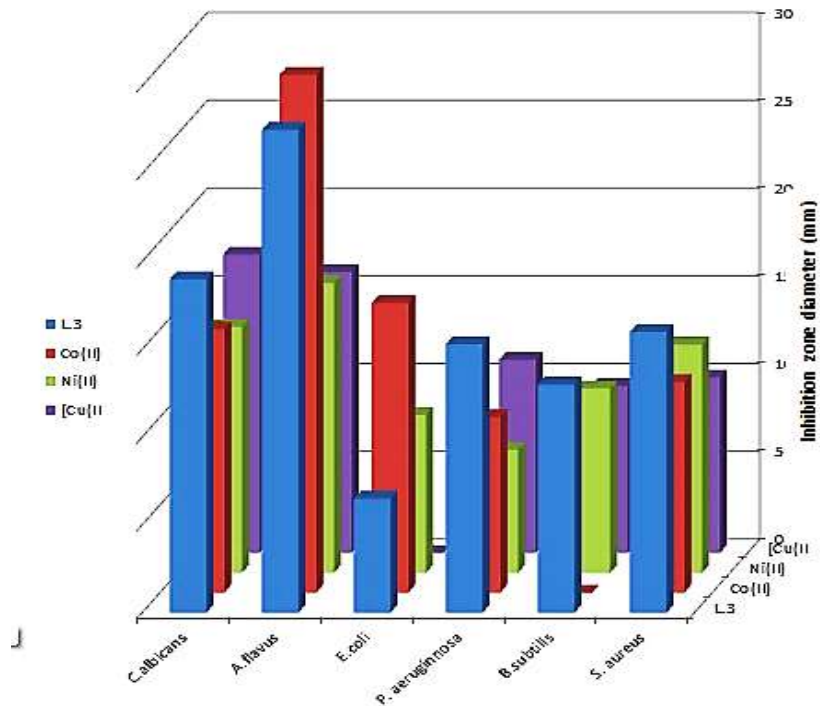
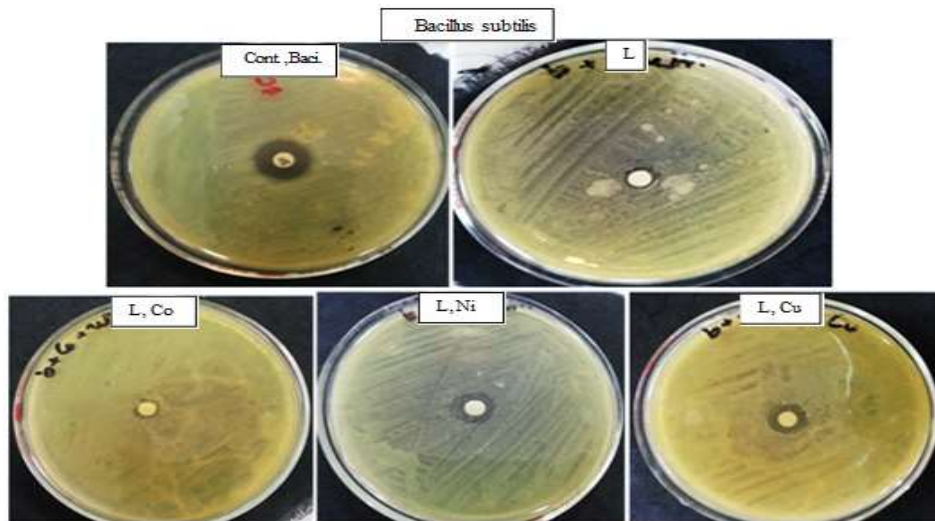
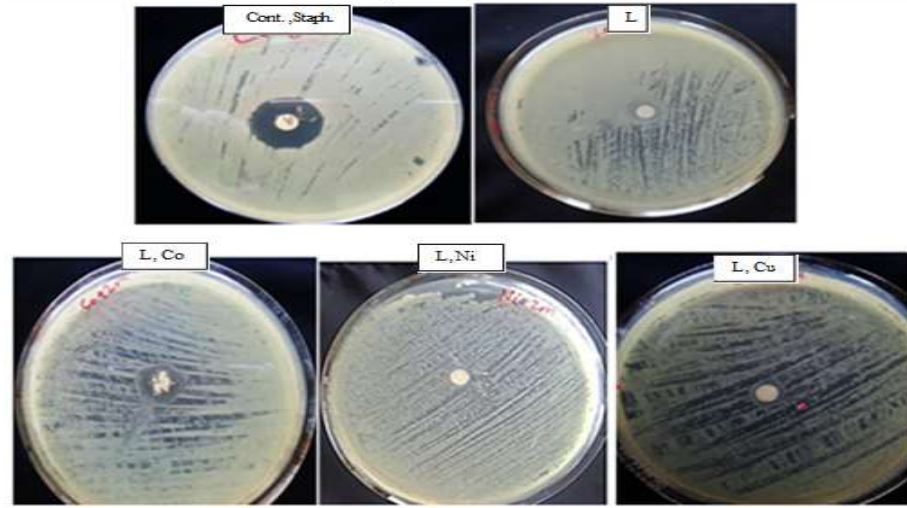


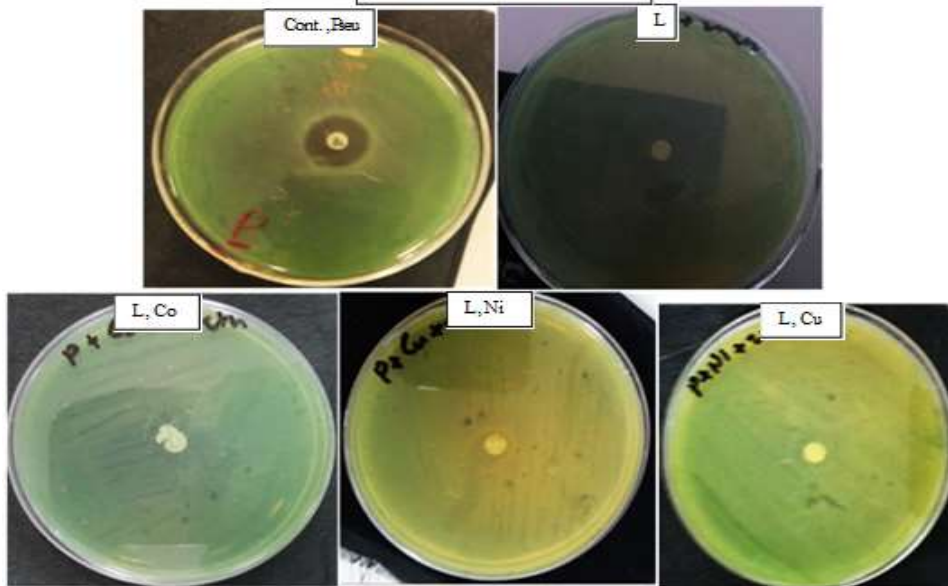
Figure 8: Diagram of the ligand and its complexes effect on the growth of bacteria and fungi (inhibition zone in mm).



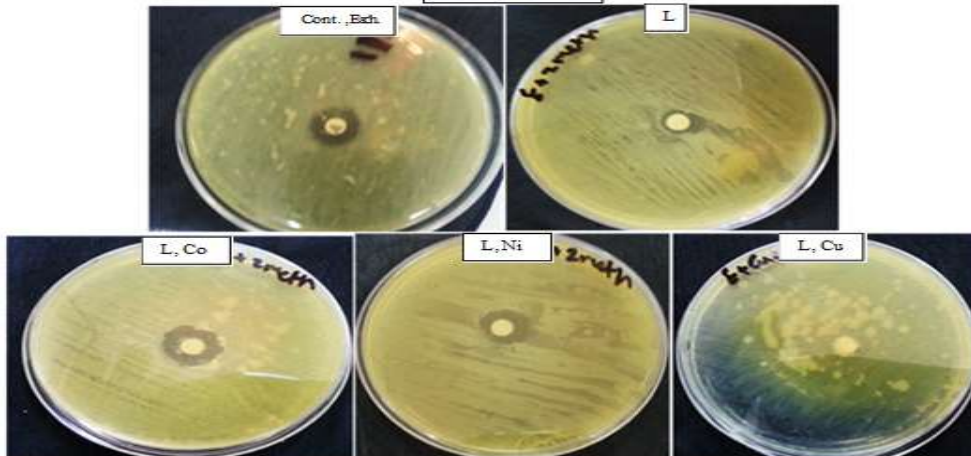
Staphylococcus aureus



Pseudomonas aeruginosa



Escherichia coli



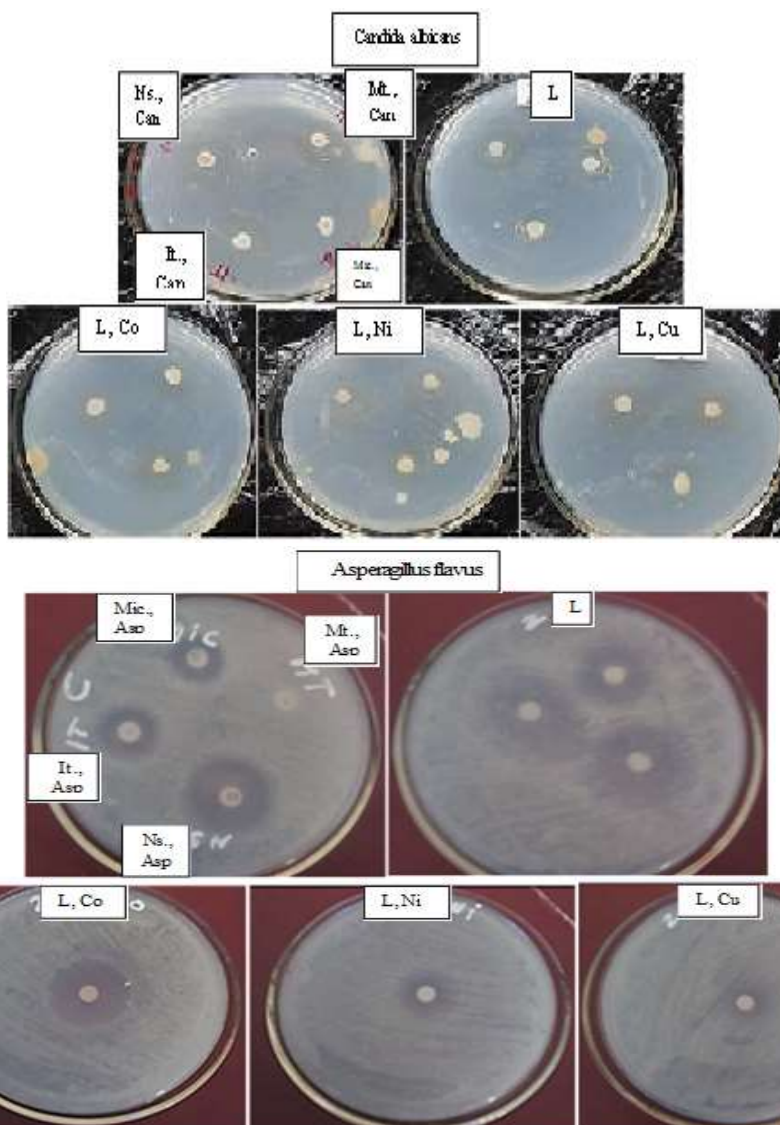


Figure 9 : Biological activity of the ligand and its complexes against microbial species

Conclusion

In this paper, new Schiff base hydrazide as a ligand obtained by the condensation reaction of 2-methoxybenzaldehyde, glycine, and hydrazine hydrate gives 2-((2-methoxybenzylidene) amino) acetohydrazide hydrate = ligand = L , which is characterized by spectral analysis. The complexation of this ligand with Co(II) , Ni(II) , and Cu(II) ions have been done. Based on the physico-chemical and spectral data discussed above, the ligand behave as a dibasic bidentate, coordinating via a nitrogen of imine and primary amine in addition to the oxygen of the carbonyl group in Ni^{II} complex. According to the elemental analysis and analytical data, we have proposed square planar geometry for Co^{II} and Ni^{II} but Cu^{II} is a distorted octahedral complex. Anti-oxidant study for the ligand reveals it good antioxidant compared with ascorbic acid which was a standard antioxidant. The X-ray study suggests a crystal system in the nano range for the ligand and its Co^{II} , Ni^{II} , and Cu^{II} complexes. Also, the ligand and complexes were tested to investigate their antimicrobial effect on some

hazardous bacterial and fungi such as *Escherichia coli*, *Staphylococcus aureus*, *Pseudomonas aeruginosa*, and *Bacillus subtilis* as bacteria in addition to *Aspergillus flavus* and *Candida albicans* as fungi. The compounds exhibited sufficient biological activity which confirms that these compounds possess antimicrobial effects

References

- [1] S. S. Shah, D. Shah, I. Khan, S. Ahmad, U. Ali, and A. Rahman, "Synthesis and Antioxidant Activities of Schiff Bases and Their Complexes," vol. 10, no. 6, pp. 6936–6963, 2020.
- [2] S. A. Dalia, F. Afsan, S. Hossain, C. M. Zakaria, and M. Ali, "A short review on chemistry of schiff base metal complexes and their catalytic application," vol. 6, no. 3, pp. 2859–2866, 2018.
- [3] M. A. Zayed, A. Belal, and S. M. A. H. Ragha, "Structure Studies of the Prepared Novel Hydrazone Schiff 's Base Complexes Using Spectroscopic , Thermal Analyses and Their Biological Activities," vol. 1, pp. 1–10, 2018.
- [4] P. Majumdar, A. Pati, M. Patra, R. K. Behera, and A. K. Behera, "Acid Hydrazides , Potent Reagents for Synthesis of Oxygen - , Nitrogen - , and / or Sulfur-Containing Heterocyclic Rings," vol. 114, pp. 2942- 2977, 2014.
- [5] S. Rv, A. P. Patel, P. T. Trivedi, G. Hr, and D. B. Khetani, "Rapid and Economic Synthesis of Schiff Base of Salicylaldehyde by Microwave Irradiation," vol. 3, no. 10, pp. 97–99, 2013.
- [6] G. Mathew, M.S. Susclan and R. Krishnan "Synthesis aand Characterization of cobalt (II) complexes of Chromen- 3- one- 3-Carboxy hydrazide and 2- (chromen - 2'- only)- 5- (aryl) 1,3,4- oxadiazole derivatives" vol. 45A, pp. 2040- 2044, 2006.
- [7] O. W. Salawu, R. A. Wuana, and J. T. Ashimom, "Synthesis , characterization and corrosion inhibition of Co (II), Ni (II), Cu (II), and Zn (II) complexes derived from nicotinic acid hydrazide," vol. 2016, pp. 2–6, 2018.
- [8] Kumar D, Kumar NM, Ghosh S, Shah K (2012) Novel bis(indolyl)hydrazide–hydrazones as potent cytotoxic agents. *Bioorg Med Chem Lett* 22:212–215
- [9] Yadagiri B, Holagunda UD, Bantu R, Nagarapu L, Guguloth V, Polepally S, Jain N (2014) Rational design, synthesis and anti-proliferative evaluation of novel benzosuberone tethered with hydrazide–hydrazones. *Bioorg Med Chem Lett* 24:5041–5044
- [10] Machakanur SS, Patil BR, Badiger DS, Bakale RP, Gudasi KB, Bligh SWA (2012) Synthesis, characterization and anticancer evaluation of novel tri-arm star shaped 1,3,5-triazine hydrazones. *J Mol Struct* 1011:121–127
- [11] Nasr T, Bondock S, Youns M (2014) Anticancer activity of new coumarin substituted hydrazide–hydrazone derivatives. *Eur J Med Chem* 76:539–548

- [12] Kumar V, Basavarajaswamy G, Rai MV, Poojary B, Pai VR, Shruthi N, Bhat M (2015) Rapid ‘one-pot’ synthesis of a novel benzimidazole-5-carboxylate and its hydrazone derivatives as potential anti-inflammatory and antimicrobial agents. *Bioorg Med Chem Lett* 25:1420–1426
- [13] Çakır B, Dağ Ö, Yıldırım E, Erol K, Şahin MF (2001) Synthesis and anticonvulsant activity of some hydrazones of 2-[(3*H*)-oxobenzoxazolin-3-yl-aceto]hydrazide. *J Fac Pharm Gazi* 18:99–106
- [14] Şenkardes S, Kaushik-Basu N, Durmaz İ, Manvar D, Basu A, Atalay R, Küçükgül ŞG (2016) Synthesis of novel diflunisal hydrazone-hydrazones as anti-hepatitis C virus agents and hepatocellular carcinoma inhibitors. *Eur J Med Chem* 10:301–308
- [15] Siddiqui AISM, Macedo TS, Moreira DRM, Leite ACL, Soares MBP, Azam A (2014) Design, synthesis and biological evaluation of 3-[4-(7-chloro-quinolin-4-yl)-piperazin-1-yl]-propionic acid hydrazones as antiprotozoal agents. *Eur J Med Chem* 75:67–76
- [16] McCalla DR, Reuvers A, Kaiser C (1970) Mode of action of nitrofurazone. *J Bacteriol* 104:1126–1134
- [17] Chatterjee SN, Ghosh S (1979) Mechanism of action of furazolidone: inter-strand cross-linking in DNA & liquid holding recovery of *Vibrio cholerae* cells. *Indian J Biochem Biophys* 16(3):125–130
- [18] Ali BH (1983) Some pharmacological and toxicological properties of furazolidone. *Vet Res Commun* 6:1–11
- [19] McOsker CC, Fitzpatrick PM (1994) Nitrofurantoin: mechanism of action and implications for resistance development in common uropathogens. *J Antimicrob Chemother* 33:23–30
- [20] Munoz-Davila MJ (2014) Role of old antibiotics in the Era of antibiotic resistance. Highlighted nitrofurantoin for the treatment of lower urinary tract infections. *Antibiotics* 3:39–48
- [21] H. Gao, “Synthesis , Characterisation and Transition Metal Ion Complexation Studies of ‘ Pocket - Like ’ Imine and Amide Derivatives,” National University of Ireland, ,December, 2013.
- [22] G. G. Mohamed and M. M. Omar, “Metal Complexes of Schiff Bases : Preparation , Characterization , and Biological Activity,” vol. 30, pp. 361–382, 2006.
- [23] A. Ghara *et al.*, “Research Article A detailed study of Transition Metal Complexes of a Schiff base with its Physico- chemical properties by using an electrochemical method,” vol. 3, no. 3, pp. 86–94, 2017.
- [24] N. Resources, “Conductometric Study of Complex Formation Between Cu(II) Ion and

- 4-Amino-3-ethyl-1, 2, 4- triazol-5-thione in Binary Ethanol / Water Mixtures,” vol. 5, no. 3, pp. 551–556, 2008.
- [25] P. Shamly, M. P. Nelson, A. Antony, J. T. Varkey, S. Teresa, and S. Albert, “Synthesis of Salicylaldehyde Based Schiff Bases and Their Metal Complexes in Aqueous Media - Characterization and Antibacterial Study,” vol. 9, pp. 26566–26570, 2018.
- [26] Neslihan Demirbas , Ahmet Demirbas And Kemalsancak, “Synthesis and Characterization of Some 3-alkyl-4-amino-5-cyanomethyl-4H-1,2,4-triazoles,” vol. 26, pp. 801–806, 2002
- [27] E. L. A. Mohamed, B. Mohamed, B. P. Zitoune, U. Moulay, and B. P. Zitoune, “Synthesis and Characterization of N-salicylidèneglycinatè (KHL) And caffeine complexes with Cd (II), Cu (II), Ni (II), Zn (II) Equipe Métallation , complexes moléculaires et applications,” vol. 3, no. 5, pp. 22–34, 2014.
- [28] G. Kumar, D. Kumar, and C. P. Singh, “Synthesis, physical characterization and antimicrobial activity of trivalent metal Schiff base complexes,” vol. 75, no. 5, pp. 629–637, 2010.
- [29] E. Ay, “Synthesis and Characterization of Schiff Base 1-Amino-4-methylpiperazine Derivatives,” vol. 12, no. 3, pp. 375–392, 2016.
- [30] D.L. Pavia, G. M. Lampman and G.S. Kriz, “Introduction of Spectroscopy”Third Edition.
- [31] G. K. Sinha, A. Priya, S. Priya, and S. Narayan, “Synthesis and Biological Activity of Some Schiff Bases from Phthalimides,” vol. 5, no. 2, pp. 36–42, 2017.
- [32] H. H. Sabah, “Synthesis , spectroscopic characterization of schiff bases derived from 4 , 4 -methylen di aniline,” vol. 6, no. 2, pp. 38–41, 2014.
- [33] Z. Yang and P. Sun, “Compare of three ways of synthesis of simple Schiff base,” pp. 12–14, 2006.
- [34] Z. S. M. Al-garawi, I. H. R. Tomi, and A. L. I. H. R. Al-daraji, “Synthesis and Characterization of New Amino Acid-Schiff Bases and Studies their Effects on the Activity of ACP , PAP and NPA Enzymes (In Vitro),” vol. 9, no. 2, pp. 962–969, 2012.
- [35] E. Canpolat, A. Ağlamiş, H. Şahal, and M. Kaya, “Some Transition Metal Complexes of NO Type Schiff Base : Preparation and Characterization,” vol. 37, no. 1, pp. 67-73, 2016.
- [36] R. F. Muslim, H. M. Tawfeeq, M. Nadhim, O. Obaid, and H. Abid, “Synthesis , characterization and evaluation of antifungal activity of seven-membered heterocycles,” vol. 56, no. 2, pp. 39–58, 2018.
- [37] Neelofar, Nauman Ali, Adnan Khan, Salma Amir, Noureen Amir Khan and

- Muhammad Bilal, "Synthesis of Schiff Bases Derived From 2-Hydroxy-1-Naphthaldehyde and Their Tin(II) Complexes for Antimicrobial and Antioxidant Activities," vol. 31, no. 3, pp. 445–456, 2018.
- [38] S. Educ, "Adiyaman University Journal of Science," vol. 7, no. June, pp. 47–59, 2017.
- [39] A. Spektrum, S. Kompleks and C. Ii, "Synthesis , Structural , Antibacterial And Spectral Studies Of Co (II) Complexes With Salicylaldehyde and P -Chloro-Benzaldehyde 4-Phenylthiosemicarbazone," Vol. 16, No. 2, Pp. 103–109, 2012.
- [40] M. M. A.- Jiboury, "Preparation , Characterization and Biological Activities of some Unsymmetrical Schiff Bases Derived from m-phenylenediamine and their Metal Complexes" vol. 28, no. 2, pp. 23–36, 2019.
- [41] M. M. Tulu and A. M. Yimer, "Catalytic Studies on Schiff Base Complexes of Co (II) and Ni (II) Using Benzoylation of Phenol," vol. 6, no. 3, 2018.
- [42] E. Yousef, "Synthesis of Co (II) and Cu (II) Complexes with NO and N₂O₂ Ligands derived from Salicylaldehyde," vol. 8, no. 7, pp. 82–93, 2016.
- [43] T. H. Mahmood and E. A. Hassan, "Preparation and Characterization of Co (II), Ni (II) and Cu (II) ions Binuclear Complexes with Macrocyclic Schiff Base Derived from Acidhydrazide and α -Hydroxy Ketone," vol. 7, no. 2, 2013.
- [44] M. S. Refat, H. M. A. Al-maydama, F. M. Al-azab, R. R. Amin, and Y. M. S. Jamil, "Molecular and Biomolecular Spectroscopy Synthesis , thermal and spectroscopic behaviors of metal – drug complexes : La (III), Ce (III), Sm (III) and Y (III) amoxicillin trihydrate antibiotic drug complexes," vol. 128, pp. 427–446, 2014.
- [45] H. M. Al-maydama, A. A. Abduljabbar, M. A. Al-maqtari, and K. M. Naji, "Study of temperature and irradiation in fl uence on the physicochemical properties of Aspirin," vol. 1157, pp. 364–373, 2018.
- [46] M. S. Refat, F. M. Al-azab, H. M. A. Al-maydama, R. R. Amin, and Y. M. S. Jamil, "Molecular and Biomolecular Spectroscopy Synthesis and in vitro microbial evaluation of La (III), Ce (III), Sm (III) and Y (III) metal complexes of vitamin B6 drug," vol. 127, pp. 196–215, 2014.
- [47] A. H. Abed, Z. T. Khodair, T. M. Al-saadi, and T. A. Al-dhahir, "Study the evaluation of Williamson – Hall (W- H) strain distribution in silver nanoparticles prepared by sol-gel method Study the Evaluation of Williamson – Hall (W-H) Strain Distribution in Silver Nanoparticles Prepared by Sol-Gel Method," 2019.
- [48] K. Mohammed, F. Hameed, A. Ahmed, E. Mohammed, Y. Mohammed, and M. Roslen, "Ferric-bipyridine assay : A novel spectrophotometric method for measurement of antioxidant capacity," vol. 6, 2020.

- [49] M. S. Refat, F. M. Al-azab, H. M. A. Al-maydama, R. R. Amin, Y. M. S. Jamil, and M. I. Kobeasy, "Molecular and Biomolecular Spectroscopy Synthesis , spectroscopic and antimicrobial studies of La (III), Ce (III), Sm (III) and Y (III) Metformin HCl chelates," vol. 142, pp. 392–404, 2015.
- [50] A. G. M. Al-daher, "New Tridentate Hydrazone Metal Complexes Derived from 2-Hydroxy-4- Methoxyacetophenone and some Acid Hydrazides : Synthesis , Characterization and Antibacterial Activity Evaluation" vol. 28, no. 2, pp. 100–111, 2019.